

Model Predictive Control of a PWM Rectifier on Unbalanced Grid Voltage Conditions

Abstract. In order to improve the DC-side voltage and AC-side current of the pulse width modulation (PWM) rectifier on unbalanced grid voltage conditions, the paper proposed a model predictive control (MPC) strategy of PWM rectifier. With no separation of the positive and negative sequence components of voltage and current, the proposed method can significantly reduce the effect of the negative sequence component and improve the dynamic response and robustness of a PWM rectifier. The experimental results validate the correction and effectiveness of the proposed method.

Streszczenie. W artykule przedstawiono opracowane sterowanie predykcyjne MPC dla prostownika MSI. Brak separacji między składowymi zgodną i przeciwną napięcia i prądu, pozwala na znaczną redukcję składowej przeciwnej, zwiększenie dynamiki odpowiedzi oraz elastyczności pracy algorytmu. Przedstawione wyniki eksperymentalne potwierdzają skuteczność działania rozwiązania. (Sterowanie predykcyjne dla prostownika MSI w warunkach niesymetryczności napięcia sieci).

Keywords: rectifier, model predictive control, unbalanced grid voltage, robustness.

Słowa kluczowe: prostownik, sterowanie predykcyjne, niesymetryczne napięcie sieci, elastyczność.

Introduction

Pulse width modulation (PWM) rectifiers have been widely used due to its advantages, such as adjustable DC-side voltage, adjustable power factor and low harmonics in AC-side current [1-4]. However, the advantages will disappear when the grid voltage is unbalanced. On the unbalanced grid voltage conditions, the oscillation occurs in the DC-side voltage and AC-side current of the PWM rectifier based on traditional vector control, which significantly deteriorates the performance of the rectifier and even results in an accidental shutdown [5]. In order to improve the performance of the PWM rectifier on unbalanced grid voltage conditions, some control methods have been presented [6]. Among the proposed methods, the most popular and widely used one is the vector control in dual synchronous frame [6]. It decouples the unbalanced PWM rectifier model into two balanced models, which are in the positive and the negative synchronous frames separately. Then it applies the traditional vector control in the dual synchronous frame separately to achieve the control of the rectifier on unbalanced grid voltage. The method is well-understood, but it also features the complicated separation of the positive and negative components, many parameters of controllers to be adjusted and weak robustness as traditional vector control.

This paper proposed a model predictive control (MPC) strategy of the PWM rectifier on unbalanced grid voltage conditions. Considering the 1st order differential equations of PWM rectifier as the predictive model, the proposed strategy achieves the control of the PWM rectifier by predicting the finite future states and optimizing the performance functions in every control cycle. It does not require the separation of the positive and negative components, features the fast dynamic response and strong robustness, and can significantly improve the DC-side voltage and AC-side current of the PWM rectifier. The experimental results validate the correction and effectiveness of the proposed strategy.

The PWM rectifier on unbalanced voltage conditions

The typical structure of 2-level 3-phase PWM rectifier is illustrated in Fig.1. In the positive synchronous frame, the AC-side mathematical model of the PWM rectifier can be written as

$$(1) \quad \begin{cases} u^{d+} = Ri^{d+} + Lp i^{d+} - \omega_c Li^{q+} + e^{d+} \\ u^{q+} = Ri^{q+} + Lp i^{q+} + \omega_c Li^{d+} + e^{q+} \end{cases}$$

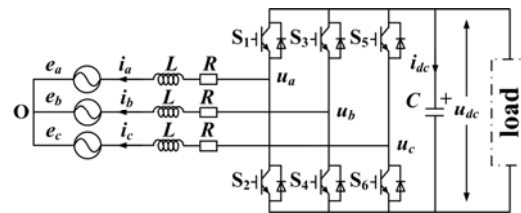


Fig.1. The typical structure of a PWM rectifier

where: u^d, u^q – AC-side output voltage on d-axis and q-axis in positive synchronous frame, e^d, e^q – grid voltage on d-axis and q-axis in positive synchronous frame, i^d, i^q – AC-side current on d-axis and q-axis in positive synchronous frame, ω_c – the synchronous radian frequency, L – AC-side inductance, R – internal resistance of the AC-side inductor, p – derivative operator. The power flows from the rectifier to the grid can be expressed as

$$(2) \quad \begin{cases} P_g = e^{d+} i^{d+} + e^{q+} i^{q+} \\ Q_g = e^{q+} i^{d+} - e^{d+} i^{q+} \end{cases}$$

where: P_g – active power, Q_g – reactive power.

The DC-side mathematical model of the PWM rectifier is

$$(3) \quad u_{dc} \dot{i}_c = u_{dc} C p u_{dc} = -P_g - \Delta P$$

where: u_{dc} – DC-side voltage, C – DC-side capacitance, ΔP – active power flow to the load. It is known from (3) that the DC-side voltage can be regulated by the AC-side active power, and from (2) the AC-side active and reactive power can be adjusted by the AC-side current. That is the principle of typical control structure of outer voltage loop and inner current loop. When the grid voltage is unbalanced, the theory of symmetrical components allows decoupling any 3-phase sinusoidal power system as 3 separate and balanced systems: positive, negative and zero sequences. Generally, the zero sequence is not considered in a 3-line system, so only the positive and negative sequences will be analyzed in this section for the convenience. Fig.2 illustrates the vector relationship among the stationary, positive synchronous and negative synchronous frames, where \bar{F} indicates the general electromagnetic vector.

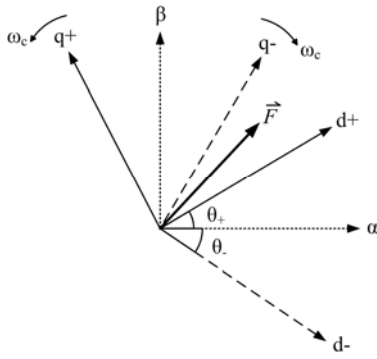


Fig.2. Vector relationship among stationary, positive and negative synchronous frames

$$(4) \quad \begin{cases} \bar{F}^{dq+} = \bar{F}^{\alpha\beta} e^{-j\omega_c t}, \bar{F}^{dq-} = \bar{F}^{\alpha\beta} e^{j\omega_c t} \\ \bar{F}^{dq+} = \bar{F}^{dq-} e^{-2j\omega_c t}, \bar{F}^{dq-} = \bar{F}^{dq+} e^{2j\omega_c t} \end{cases}$$

where: \bar{F}^{dq+} – the vector in positive synchronous frame, \bar{F}^{dq-} – the vector in negative synchronous frame, $\bar{F}^{\alpha\beta}$ – the vector in stationary frame, t – time.

Once the grid voltage is unbalanced, the negative sequence component of the electromagnetic vector will occur. Then the AC-side output voltage and current of the PWM rectifier can be known from (4) that

$$(5) \quad \begin{cases} u^{d+} = u_+^{d+} + u_-^{d+} = u_+^{d+} + u_-^{d-} \cos \theta + u_-^{q-} \sin \theta \\ u^{q+} = u_+^{q+} + u_-^{q+} = u_+^{q+} + u_-^{q-} \cos \theta - u_-^{d-} \sin \theta \end{cases}$$

$$(6) \quad \begin{cases} i^{d+} = i_+^{d+} + i_-^{d+} = i_+^{d+} + i_-^{d-} \cos \theta + i_-^{q-} \sin \theta \\ i^{q+} = i_+^{q+} + i_-^{q+} = i_+^{q+} + i_-^{q-} \cos \theta - i_-^{d-} \sin \theta \end{cases}$$

where the subscript “+” and “-” indicate the positive and negative sequence components respectively, and θ is the angle between d+ axis and d- axis, which can be regarded as $2\omega_c t$. Substitute (5) and (6) into (2), the AC-side power can be rewritten as

$$(7) \quad \begin{cases} P_g = P_{g0} + P_{g2\omega} \\ Q_g = Q_{g0} + Q_{g2\omega} \end{cases}$$

where:

$$\begin{aligned} P_{g0} &= u_+^{d+} i_+^{d+} + u_+^{q+} i_+^{q+} + u_-^{d-} i_-^{d-} + u_-^{q-} i_-^{q-} \\ P_{g2\omega} &= (u_+^{d+} i_-^{d-} + u_+^{q+} i_-^{q-} + u_-^{d-} i_+^{d+} + u_-^{q-} i_+^{q+}) \cos \theta \\ &\quad + (u_+^{d+} i_-^{q-} - u_+^{q+} i_-^{d-} - u_-^{d-} i_+^{q+} + u_-^{q-} i_+^{d+}) \sin \theta \\ Q_{g0} &= u_+^{q+} i_+^{d+} - u_+^{d+} i_+^{q+} + u_-^{q-} i_-^{d-} - u_-^{d-} i_-^{q-} \\ Q_{g2\omega} &= (u_+^{q+} i_-^{d-} + u_+^{d+} i_-^{q-} - u_-^{d+} i_+^{q-} - u_-^{q+} i_+^{d+}) \cos \theta \\ &\quad + (u_+^{q+} i_-^{q-} - u_-^{d-} i_+^{d+} + u_+^{d+} i_-^{d-} - u_-^{q-} i_+^{q+}) \sin \theta \end{aligned}$$

When grid voltage is unbalanced and no proper method is used, (6) indicates large harmonics will occur in the AC-side current, and (7) indicates oscillation at double synchronous frequency will occur in the AC-side power, resulting in the oscillation in the DC-side voltage according to (3). Those above will significantly deteriorate the performance of the PWM rectifier, reduce the life of equipment and even permanently damage the hardware, which is the main challenge for PWM rectifier to work on unbalanced grid voltage conditions.

The model predictive control of a PWM rectifier

According to the analysis in Section II, restraining the effect of the non-positive components is the key point for the control of a PWM rectifier on unbalanced grid voltage conditions. To improve the performance of the PWM rectifier on unbalanced grid voltage conditions, a MPC method will be given in detail in this section.

Assuming that T_s is the sample period of the AC-side current loop and the sample period is the control period for the current loop, (1) can be rewritten in a discrete expression as

$$(8) \quad \begin{cases} i^{d+}(k+1|k) = ai^{d+}(k) + bi^{q+}(k) + cu^{d+}(k) - ce^{d+}(k) \\ i^{q+}(k+1|k) = ai^{q+}(k) - bi^{d+}(k) + cu^{q+}(k) - ce^{q+}(k) \end{cases}$$

where: $i^{dq+}(k+1|k)$ – the AC-side current at $(k+1)T_s$ instant, which is predicted at kT_s instant, $i^{dq+}(k)$ – the sample value of AC-side current at kT_s instant, $u^{dq+}(k)$ – the AC-side output voltage at kT_s instant, $e^{dq+}(k)$ – the sample value of grid voltage at kT_s instant, a, b, c – the parameters of the predictive model, which are defined as

$$a = 1 - T_s R / L, \quad b = T_s \omega_c, \quad c = T_s / L$$

Equation (8) can be regarded as the predictive model of the AC-side current. It indicates: if the AC-side current, AC-side output voltage and grid voltage are known at kT_s , the AC-side current at $(k+1)T_s$ can be predicted.

However, affected by the inherent control delay of the digital control chips, the practical prediction in the proposed method is made in the following way.

At kT_s , the digital processor gets the sample values of the system and obtains the control output $u^{dq+}(k)$, but the control output will not be imposed on the rectifier immediately until the digital processor updates its PWM generators at the next sample instant $(k+1)T_s$. Therefore, during the period between kT_s and $(k+1)T_s$, the rectifier is controlled by the control voltage $u^{dq+}(k-1)$ practically but not by $u^{dq+}(k)$. To eliminate the effect of control delay involved by digital micro processor, two-step forward prediction is made at kT_s according to (8). They are

$$(9) \quad \begin{cases} i^{d+}(k+1|k) = i_0^{d+}(k+1|k) \\ i^{q+}(k+1|k) = i_0^{q+}(k+1|k) \end{cases}$$

$$(10) \quad \begin{cases} i^{d+}(k+2|k) = i_0^{d+}(k+2|k) + c\Delta u^{d+}(k) \\ i^{q+}(k+2|k) = i_0^{q+}(k+2|k) + c\Delta u^{q+}(k) \end{cases}$$

where:

$$\begin{aligned} i_0^{d+}(k+1|k) &= ai^{d+}(k) + bi^{q+}(k) + cu^{d+}(k-1) - ce^{d+}(k) \\ i_0^{q+}(k+1|k) &= ai^{q+}(k) - bi^{d+}(k) + cu^{q+}(k-1) - ce^{q+}(k) \\ i_0^{d+}(k+2|k) &= ai^{d+}(k+1|k) + bi^{q+}(k+1|k) \\ &\quad + cu^{d+}(k-1) - ce^{d+}(k+1|k) \\ i_0^{q+}(k+2|k) &= ai^{q+}(k+1|k) - bi^{d+}(k+1|k) \\ &\quad + cu^{q+}(k-1) - ce^{q+}(k+1|k) \\ \Delta u^{d+}(k) &= u^{d+}(k) - u^{d+}(k-1) \\ \Delta u^{q+}(k) &= u^{q+}(k) - u^{q+}(k-1) \end{aligned}$$

The predictive model, presented by (9) and (10), is an open-loop model. It depends on the accurate system parameters and is affected by the non-ideal factors, such as random disturbance and noise. To improve the robustness of the algorithm, the feedback correction items are added to (9) and (10) as following.

$$(11) \quad \begin{cases} i_m^{d+}(k+1|k) = i^{d+}(k+1|k) + x^{d+}(k) \\ i_m^{q+}(k+1|k) = i^{q+}(k+1|k) + x^{q+}(k) \end{cases}$$

$$(12) \quad \begin{cases} i_m^{d+}(k+2|k) = i^{d+}(k+2|k) + x^{d+}(k) \\ i_m^{q+}(k+2|k) = i^{q+}(k+2|k) + x^{q+}(k) \end{cases}$$

where $x^{d+}(k)$ and $x^{q+}(k)$ are the feedback correction items. They are defined by difference between the sample current values at kT_s and the predictive current values for kT_s as following.

$$(13) \quad \begin{cases} x^{d+}(k) = f_1 \cdot [i^{d+}(k) - i^{d+}(k|k-1)] \\ x^{q+}(k) = f_2 \cdot [i^{q+}(k) - i^{q+}(k|k-1)] \end{cases}$$

where: f_1, f_2 – the coefficients of correction.

At kT_s instant, the control objective of MPC-based current loop is to reduce the error between the current reference and current prediction for $(k+2)T_s$ as much as possible, but change the AC-side output voltage as little as possible. Therefore, the performance function is given as

$$(14) \quad J(k) = \varepsilon_1 [i^{d+*}(k) - i_m^{d+}(k+2|k)]^2 + \varepsilon_2 [i^{q+*}(k) - i_m^{q+}(k+2|k)]^2 + \lambda_1 \Delta u^{d^2}(k) + \lambda_2 \Delta u^{q^2}(k)$$

where: $i^{d+*}(k)$ – the current reference, $\varepsilon_1, \varepsilon_2$ – the weight coefficients of current errors, λ_1, λ_2 – the weight coefficients of output voltage variations. Minimize the performance function, and the optimal variations of AC-side output voltage can be obtained as

$$(15) \quad \begin{cases} \Delta u^d(k) = \frac{c\varepsilon_1}{c^2\varepsilon_1 + \lambda_1} [i^{d+*}(k) - i_0^d(k+2|k) - x^d(k)] \\ \Delta u^q(k) = \frac{c\varepsilon_2}{c^2\varepsilon_2 + \lambda_2} [i^{q+*}(k) - i_0^q(k+2|k) - x^q(k)] \end{cases}$$

Generally, the bandwidth of outer loop should be smaller than the one of inner loop. Therefore the control cycle of DC-side voltage loop is given as

$$(16) \quad T = nT_s \quad (n > 1)$$

where: n – the coefficient relative to bandwidth of DC-side voltage loop. For the convenience of derivation, (3) can be rewritten as

$$(17) \quad \frac{1}{2} C p u_{dc}^2 = -P_g - \Delta P$$

According to (16) and neglecting the item of ΔP as an interrupt from the load, (17) can be written in a discrete expression as

$$(18) \quad u_{dc}^2(k+1|k) = u_{dc0}^2(k+1|k) - h\Delta P_g(k)$$

where:

$$u_{dc0}^2(k+1|k) = u_{dc}^2(k) - hP_g(k-1)$$

$$\Delta P_g(k) = P_g(k) - P_g(k-1)$$

$$h = \frac{2T}{C}$$

For the bandwidth of the DC-side voltage loop is smaller than the one of the AC-side current loop, the control delay involved by the digital micro processor can be neglected. However, similar to the predictive model of AC-side current, the feedback correction item is required to be added to (18) to improve the robustness of the system.

$$(19) \quad u_{dcm}^2(k+1|k) = u_{dc}^2(k+1|k) + y(k)$$

where $y(k)$ is the feedback correction item. It is defined by difference between the sample voltage value at kT and the predictive voltage value for kT as following.

$$(20) \quad y(k) = j \cdot [u_{dc}^2(k) - u_{dc}^2(k|k-1)]$$

where: j – the coefficients of correction.

At kT instant, the control objective of MPC-based voltage loop is to reduce the error between the voltage reference and the voltage prediction for kT as much as possible, and change AC-side active power as little as possible. Therefore, the performance function is given as

$$(21) \quad W(k) = \varepsilon_3 [u_{dc}^{*2}(k) - u_{dcm}^2(k+1|k)]^2 + \lambda_3 \Delta P_g^2$$

where: $u_{dc}^*(k)$ – the voltage reference, ε_3 – the weight coefficient relative to voltage error, λ_3 – the weight coefficient of AC-side active power variations.

Minimize the performance function, and the optimal variation of AC-side active power can be obtained as

$$(22) \quad \Delta P_g(k) = \frac{-h\varepsilon_3}{h^2\varepsilon_3 + \lambda_3} [u_{dc}^{*2}(k) - u_{dc0}^2(k+1|k) - y(k)]$$

It can be seen that the DC-side voltage loop provides the AC-side active power reference as its output, but the AC-side current loop requires the current reference. Therefore, the relationship between AC-side power and AC-side current is required to be known. The transformation equations can be obtained from (2) as

$$(23) \quad F(P_g, Q_g) : \begin{cases} i^{d+} = \frac{e^{d+} P_g + e^{q+} Q_g}{e^{d+2} + e^{q+2}} \\ i^{q+} = \frac{e^{q+} P_g - e^{d+} Q_g}{e^{d+2} + e^{q+2}} \end{cases}$$

Then the DC-side voltage loop and the AC-side current loop can cooperate with each other and the control diagram of the proposed MPC method is illustrated in Fig.3.

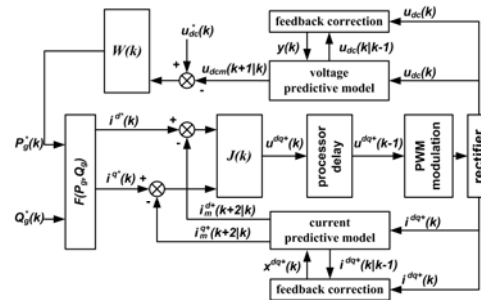


Fig.3. The control diagram of the proposed MPC strategy

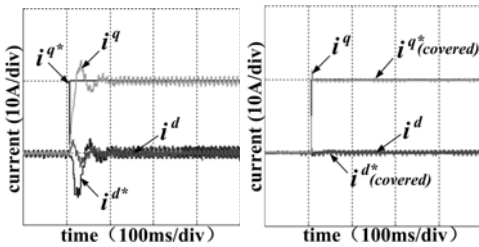
Experimental results and analysis

To validate the proposed MPC strategy, a number of tests have been carried out on a PWM rectifier system. The main parameters of the PWM rectifier are shown as Table 1. In the experiments, a 3-phase 4-line unbalanced voltage simulator is used to generate the unbalanced grid voltage. The experimental results are shown as Fig.4 – Fig.6.

Fig.4 shows the dynamic response of the current loops based on the traditional method and the proposed method respectively on normal grid conditions. For the traditional

Table 1. The parameters of the tested PWM rectifier

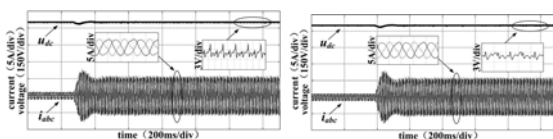
Rated grid line voltage	380 V
DC-side voltage	650 V
AC-side inductance	8 mH
DC-side capacitance	3.3 mF
DC-side load	250 Ω
Switching frequency	5 kHz



a. PI-based current loop b. MPC-based current loop
Fig.4. The step response of traditional and proposed current loops

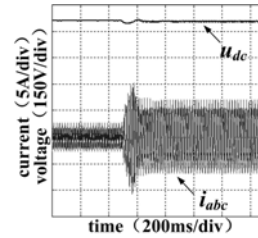
method shown as Fig.4.a, it responds the step reference with about 80ms delay, obvious overshoot and obvious influence between d-axis current and q-axis current, which is a typical PI response. In Fig.4.b, the proposed MPC-based current loop responds the step reference with only a few switching period delay, little overshoot and little influence between current on d-axis and q-axis, which benefits from the optimal control of the proposed MPC in every control cycle as derived in Section III.

Fig.5 illustrates a sudden load test when Phase C of grid voltage reduces to 50% of normal voltage. Fig.5.a and Fig.5.b indicate that the proposed method provides faster dynamic response of DC-side voltage and less overshoot of AC-side current than the traditional vector control method does. In the traditional method shown as Fig.5.b-d, the oscillation at double synchronous frequency occurs in the DC-side voltage and a number of harmonics occur in the AC-side current. They are caused by the unbalanced grid voltage and significantly deteriorate the performance of the PWM rectifier. In the proposed method shown as Fig.5.f-h, the oscillation in the DC-side voltage is reduced and the harmonics in the AC-side current is improved obviously. The contrast experimental results indicate the proposed method can restrain the effect of the non-positive sequence components of the unbalanced grid voltage and improve the dynamic and steady performance of the PWM rectifier significantly. Fig.6 shows the performance of PWM rectifier with different errors of the AC-side inductance on unbalanced grid voltage. The error degree of AC-side inductance is defined as (24).

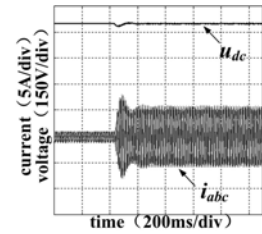


a. error degree of AC-side inductance is -20%
b. error degree of AC-side inductance is +20%

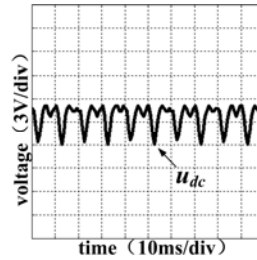
Fig.5. The experimental results of a sudden load test (Phase C of grid voltage reduced to 50% of normal voltage)



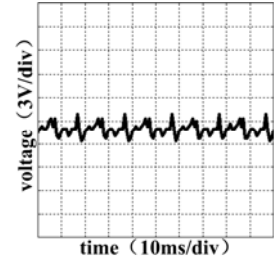
b. zoom of steady DC voltage (the traditional method)



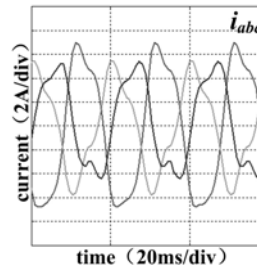
f. zoom of steady DC voltage (the proposed method)



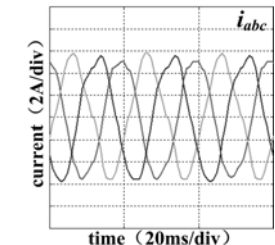
b. zoom of steady DC voltage (the traditional method)



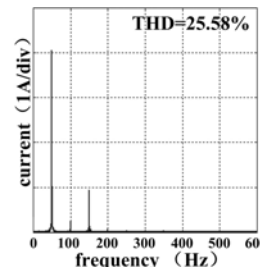
f. zoom of steady DC voltage (the proposed method)



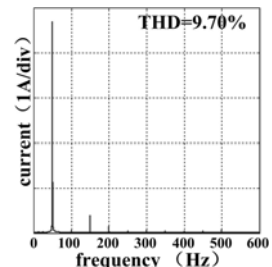
c. zoom of steady current (the traditional method)



g. zoom of steady current (the proposed method)



d. FFT of current on Phase C (the traditional method)



h. FFT of current on Phase C (the proposed method)

Fig.6. The experimental results of a sudden load test with different inductance errors (Phase C of grid voltage reduced to 50% of normal voltage)

$$(24) \quad \sigma = \frac{L_x - L}{L} \times 100\%$$

where: σ – the error degree of inductance; L – the inductance in practical system; L_x – the inductance used in control algorithm. It can be seen in Fig.6 that the -20% and +20% error degree of inductance does not make obvious influence on the dynamic performance, neither on the steady performance. It indicates the strong robustness of the proposed method.

Conclusion

This paper proposed a MPC strategy for PWM rectifier on unbalanced grid voltage conditions. The proposed method is based on the 1st order equations of PWM rectifier. Taking control delay of digital micro processor into consideration, it establishes the predictive model with feedback correction. It does not require the separation of the positive and negative components, and can control

them effectively in the positive synchronous frame by optimizing the performance functions in every control cycle. In contrast to traditional vector control, the experimental results show the proposed method for PWM rectifier can restrain the effect of the unbalanced grid voltage, reduce the oscillation in DC-side voltage and the harmonics in AC-side current, and improve the dynamic response and robustness significantly. All these factors make the proposed MPC method an attractive proposition that ensures the high-performance control and the grid-faults ride-through of PWM rectifiers.

REFERENCES

- [1] Tazil M, Kumar V, Bansal R C, et al, Three-phase double fed induction generators: an overview, IET Electric Power Application, 2010, 4(2), 75-89
- [2] Enjeti P.N., Choudhury S.A., A new control strategy to improve the performance of a PWM AC to DC converter under unbalanced operating conditions. IEEE transactions on Power Electronics, 1993,8(4),493-500
- [3] Li Yongdong, Digital control system of AC motor, Beijing: China machine press, 2003
- [4] Li Yongdong, Xiao Xi, Gao Yue, High-capacity multi-level converters, Beijing: Science press, 2005
- [5] Hu J.B., Xu L., Improved control of DFIG systems during network unbalance using PI-R current regulators, IEEE Transactions on Industrial Electronics, 2009, 56(2), 439-451
- [6] Yin B., Oruganti R., Panda S.K., et al, An output-power-control strategy for a three-phase PWM rectifier under unbalanced supply conditions, IEEE Transactions on Industrial Electronics, 2008, 55(5), 2140-2151

MA Hongwei: PhD student. Room 2-302, West Main Building, Tsinghua University, Beijing, China, 100086, E-mail: mhw08@mails.tsinghua.edu.cn.

LI Yongdong: Professor, PhD supervisor. Room 2-304, West Main Building, Tsinghua University, Beijing, China, 100086, E-mail: liyd@mail.tsinghua.edu.cn.

ZHENG Zedong: Research assistant. Room 3-302, West Main Building, Tsinghua University, Beijing, China, 100086, E-mail: zheng99@mails.tsinghua.edu.cn.

XU Lie: Research assistant. Room 3-302, West Main Building, Tsinghua University, Beijing, China, 100086, E-mail: xulie@mail.tsinghua.edu.cn.